Bandwidth enhancement of second-harmonic generation with quadratic spatial-soliton generation versus conventional methods

M. Ohkawa,* R. A. Fuerst, and G. I. Stegeman

Center for Research and Education in Optics and Lasers (CREOL), University of Central Florida, 4000 Central Florida Boulevard, Orlando, Florida 32816-2700

Received May 12, 1998; revised manuscript received August 14, 1998

A detailed numerical comparison of the bandwidth–efficiency trade-off for second-harmonic generation (SHG) achieved by the formation of two-dimensional quadratic spatial solitons versus the more conventional method of gentle focusing in the middle of a nonlinear crystal is presented. Numerical simulations for type II SHG in potassium titanyl phosphate with constant wave-vector mismatch show that the 3-dB drop-off in SHG conversion efficiency can be many multiples of π in detuning from the phase-match condition over a large range of walk-off angles and focal positions. © 1998 Optical Society of America [S0740-3224(98)01911-0]

OCIS codes: 190.0190, 190.2620, 190.5530, 140.3300.

1. INTRODUCTION

Second-harmonic generation (SHG) has been important for generating new wavelengths since the inception of nonlinear optics.[1] For example, it is being used for the generation of coherent short-wavelength light that enables an increase in the storage density of optical memories.[2] Recently, second-order nonlinear optics has found a new direction because of revived interest in cascading, a technique for mimicking third-order nonlinearities that has already demonstrated potential applications, such as optical switching, spatial-soliton formation, beam cleanup, and so on.[3] Of particular interest here is the formation of quadratic solitons, which occurs during SHG under conditions quite different from the usual ones used for conventional SHG.[4] It has been shown that when a threshold input intensity for an input fundamental beam diameter is surpassed, strong coupling occurs between the fundamental and second harmonic generated, and the beams lock to produce a soliton that propagates without spatial diffraction. This soliton contains both the fundamental and harmonic in a specific intensity ratio, and, for fundamental only, some energy is lost to radiation fields.[4,5] For efficient SHG this limits the fraction of energy converted into the harmonic. On the other hand, the process is very robust, in keeping with the general properties of solitons. The trade-off between the advantages of soliton formation and conventional SHG is examined in this paper.

This study uses numerical experiments to compare the characteristics of the SHG resulting from the dynamic process of quadratic spatial-soliton formation and the conventional setup in which slowly diffracting fundamental beams are focused at the center of a homogeneous crystal for optimal conversion to the second harmonic. Comparisons are made based on the most important parameters for SHG including phase mismatch (owing to birefringent and temperature tuning), spatial walk-off, and focusing tolerances on the conversion efficiency.

2. NUMERICAL SIMULATION OF SECOND-HARMONIC GENERATION

The characteristics of SHG, e.g., the phase-matching condition and conversion efficiency, depend on the detailed properties of the noncentrosymmetric nonlinear medium. The numerical simulations are based on common doubling crystal potassium titanyl phosphate. It has an effective d coefficient reported as large as 3.0 pm/V for type II SHG at near-infrared fundamental wavelengths,[6] and it has been demonstrated experimentally to support spatial-soliton formation.[4] In a type II SHG interaction, three beams are involved, that is, two orthogonally polarized fundamental waves and one extraordinarily polarized second-harmonic wave. The interaction is described by three coupled-mode equations:

$$\frac{\partial A_1}{\partial z} + \frac{1}{2ik_1}\left(\frac{\partial^2 A_1}{\partial x^2} + \frac{\partial^2 A_1}{\partial y^2}\right) = i\Gamma A_2^* A_3 \exp(-i\Delta k z),$$

$$\frac{\partial A_2}{\partial z} - \rho_\omega \frac{\partial A_2}{\partial x} + \frac{1}{2ik_2}\left(\frac{\partial^2 A_2}{\partial x^2} + \frac{\partial^2 A_2}{\partial y^2}\right) = i\Gamma A_1^* A_3 \exp(-i\Delta k z),$$

$$\frac{\partial A_3}{\partial z} - \rho_{2\omega} \frac{\partial A_3}{\partial x} + \frac{1}{2ik_3}\left(\frac{\partial^2 A_3}{\partial x^2} + \frac{\partial^2 A_3}{\partial y^2}\right) = 2i\Gamma A_1 A_2 \exp(i\Delta k z), \quad (1)$$

where A_1 and A_2 are the envelopes of the two fundamental waves and A_3 is the envelope of the second-harmonic wave; ρ_ω (0.188 deg) and $\rho_{2\omega}$ (0.276 deg) are the walk-off angles of the extraordinary fundamental and second-

0740-3224/98/112769-04$15.00

harmonic, respectively. Γ is the nonlinear coupling coefficient, and Δk is the wave-vector mismatch.

For the above system of equations, analytic solutions cannot be derived in many cases, and it is useful to deal with this problem by use of numerical methods. The same two-dimensional beam-propagation method was used to evaluate SHG with and without soliton formation. The $x-y$ plane was chosen normal to the beam-propagation direction (z axis) and was divided into a numerical grid of 256 by 256 points. The 15 points nearest the outermost boundaries were used as a matched absorption filter to avoid reflections of radiation fields from the boundaries. The fundamental and second-harmonic waves were propagated in a stepwise fashion in the crystal and reached the output face after 500 or 1500 steps from the entrance face. In each half-step, linear propagation was calculated with a fast-Fourier-transform algorithm in Fourier space, followed by computation of the nonlinear propagation with the second-order Runge Kutta algorithm.[7] The crystal length was assumed to be 10.8 mm, which corresponded to five diffraction lengths for a focused beam with a 20-μm waist. This was chosen to closely model the experimental situations already realized.

3. RESULTING CONVERSION EFFICIENCY FOR BOTH TYPES OF SECOND-HARMONIC GENERATION

A. Dependence on Phase Mismatch

It is well known that for conventional SHG the conversion efficiency is critically dependent on phase mismatch. In soliton formation the phase mismatch also affects the resulting interaction of the three beams so that the composition of the solitons and the threshold for formation of the soliton changes.[5,8] We first describe the relation between conversion efficiency and phase mismatch for the two cases. For the conventional SHG case, four different fundamental beam waists of 20, 100, 200, and 500 μm were focused at the center of the crystal corresponding (at constant power) to peak input intensities of 5, 0.2, 0.05, and 0.008 GW/cm^2 for each of the two orthogonally polarized fundamental waves, respectively. For the quadratic soliton case the input fundamental beams were focused to 20 μm at the entrance face of the crystal with a peak intensity of 7.5 GW/cm^2 in each polarization.

Figure 1 shows the conversion efficiency as a function of phase mismatch for both cases. The SHG soliton efficiency varied by only 15% to 20% over the phase-mismatch range of -2π to $+2\pi$. It follows from Fig. 2 that the detuning bandwidth of the conversion with the fundamental focused onto the front face can be as large as 15π. The sharp efficiency drop off on the negative side of phase match is caused by the increasing threshold for soliton formation.[8] For positive detuning, the self-focusing effect from cascading leads to a very slow roll-off with detuning. For higher input fundamental powers the drop in efficiency with detuning is even slower.

In conventional SHG the well-known variations in the efficiency with phase mismatch depend on both the beam waist and the input power of the fundamental beams.

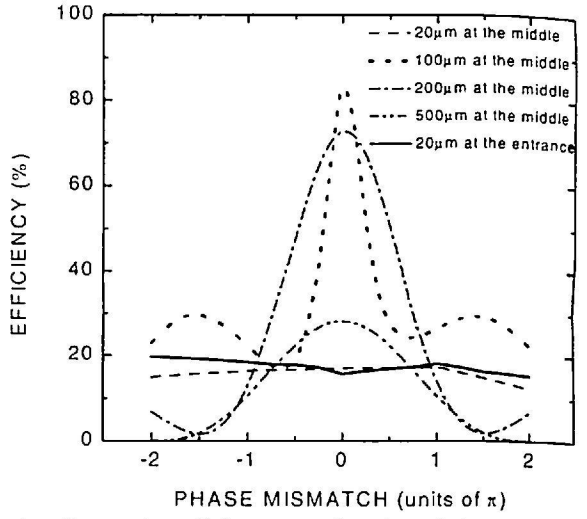

Fig. 1. Conversion efficiency as a function of phase mismatch. For the solid curve, the input beams were 20 μm at the entrance face of the crystal with the peak intensity of each input fundamental beam set to 7.5 GW/cm^2. The other curves indicate conventional SHG with the input beams focused at the center of the crystal. There are four different beam waists corresponding to 20, 100, 200, and 500 μm with peak intensities of 5, 0.2, 0.05, and 0.008 GW/cm^2, respectively.

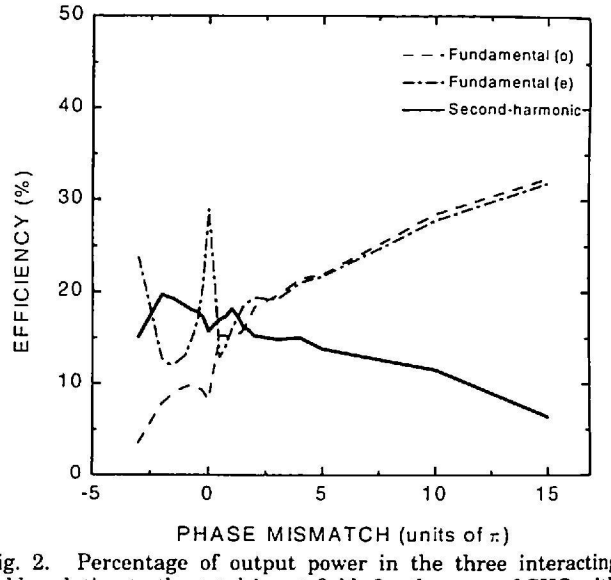

Fig. 2. Percentage of output power in the three interacting fields relative to the total input field, for the case of SHG with solitons. The peak fundamental powers were 7.5 GW/cm^2.

Figure 1 illustrates that for a beam waist of 100 μm a peak conversion efficiency in excess of 90% had a bandwidth of only 0.6π. For a larger spot (500 μm) at the focal position the variation in efficiency followed the classic sinc-like function, which can be analytically derived under the assumption of a nondepleted fundamental pump beam. The conventional focusing condition for a beam waist of 20 μm at the center of the crystal proved to be very interesting: the efficiency dropped below 20%, near the conversion efficiency for soliton formation, regardless of the very high peak power of the input beams. This occurs because the strong interaction between the three fields almost causes a soliton to form. However, a soliton was not generated since the threshold was higher than the 5 GW/cm^2 in each fundamental input because of the

limited length of interaction between the strong fields, i.e., the process did not start until about midway through the crystal.

The very broad detuning bandwidth available with solitons is a very attractive feature for SHG. The resulting tolerances on angular (or temperature) control are greatly increased over the conventional SHG approach. However, the price for this attractive feature is a reduction in the maximum SHG conversion efficiency that can be achieved relative to the conventional case. Note that the relative fractions of the three solitonic fields change with phase mismatch. This feature can be useful for applications where the fundamental and second-harmonic waves are both used, for example, in further parametric interactions such as sum-frequency generation to produce a third-harmonic wave.

B. Dependence on Conversion Efficiency on Walk-Off Angle

Spatial walk-off also affects the conversion efficiency of conventional SHG although its influence is often neglected when an analytical solution is derived.[9] In potassium titanyl phosphate we considered the case where one fundamental and the second-harmonic are ordinarily polarized while the other fundamental is extraordinarily polarized, which occurs for type II SHG phase matched in the x–z plane above 1078 nm. The extraordinary, fundamental-beam walk-off angle depends on its wavelength. In this series of simulations the phase mismatch was assumed to be zero, and the walk-off angle was changed from 0 to 0.9 deg as a function of fundamental wavelength. The peak intensities (at constant power) were 10, 0.4, 0.1, and 0.016 GW/cm^2 for input beam waists of 20, 100, 200, and 500 μm, respectively.

Figure 3 shows the conversion efficiency versus walk-off angle for both the conventional and the soliton-generated second harmonic. For the soliton case the efficiency was fairly constant at 18% for walk-off angles of 0 to 0.9 deg. When the peak input intensity was increased, the maximum walk-off angle for maintaining soliton formation also increases. The SHG efficiency in the conventional case depends strongly on the walk-off angle for a 100-μm input-beam waist at the crystal's center. The maximum offset in the beam positions possible for a 1-cm-long crystal is ~150 μm, so input beams larger than this do not suffer significantly from walk-off (although some output-beam distortion may occur). If the fundamental beams were focused to 20 μm at the center, the efficiency dropped below 20%. In the case of small walk-off angles, soliton formation occurs in the crystal for this tightly focused beam near the crystal's center so that the efficiency was ~18%. For large walk-off angles the efficiency decreases with increasing walk-off angle because there was not a strong enough interaction.

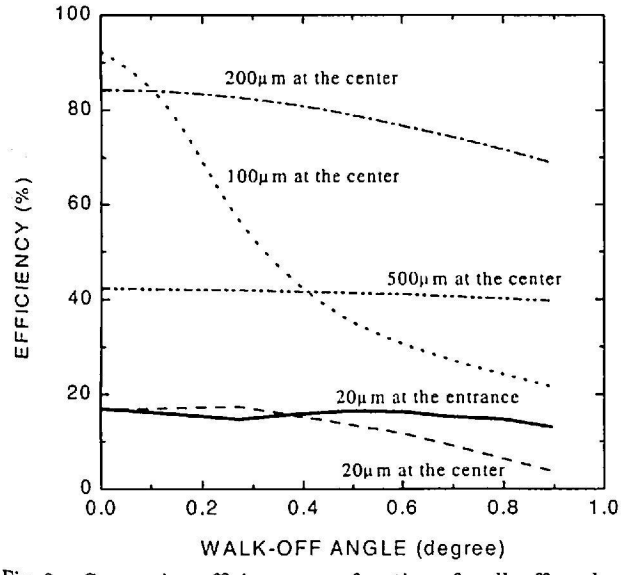

Fig. 3. Conversion efficiency as a function of walk-off angle of the extraordinary polarized fundamental field at phase match. The peak input intensity of each fundamental was 10, 0.4, 0.1, and 0.016 GW/cm^2 for 20-, 100-, 200-, and 500-μm beam waists, respectively.

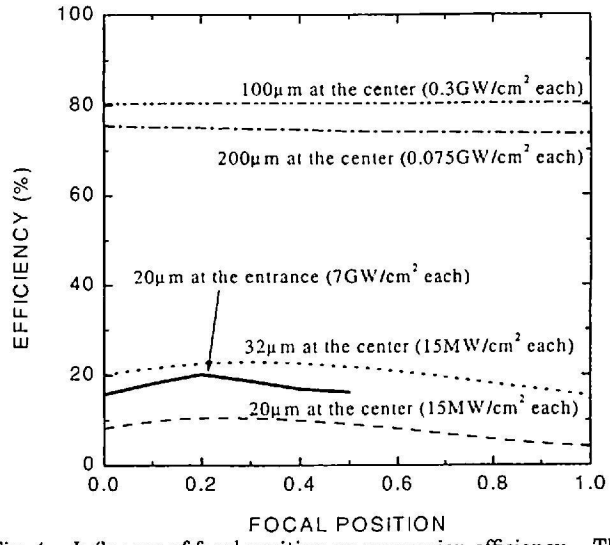

Fig. 4. Influence of focal position on conversion efficiency. The solid curve identifies SHG with spatial-soliton formation. The other traces illustrate the efficiency as a function of focal position for conventional SHG.

C. Dependence of Focal Position

In this subsection we again consider phase-matched SHG at 1064 nm to evaluate the dependence of soliton generation on the focal position of the input beam. Figure 4 shows the influence on conversion efficiency of the position at which the input fundamental beam would be focused in the absence of SHG. In the figure, there are five curves for three focusing conditions: focusing tight enough to form a soliton (solid curve), loose focusing at high input power (dot–dash curve and dash–dot–dot curve), and tight focusing at low input powers (dash curve and dot curve). Zero and one in the figure correspond to the input and the output faces, respectively. In general, the SHG efficiency is only weakly dependent on the focal position for all of the cases examined. For soliton formation the threshold increases when the focal position is placed near the center of the crystal. At the peak intensity of 7 GW/cm^2 for each of the orthogonally polarized fundamental beams, the soliton formation is possible even if the focal position is located anywhere between the entrance face and the crystal center.

4. PROFILES OF OUTPUT BEAMS

An almost Gaussian spatial profile is often favorable for applications of SHG, especially for coupling into waveguides or optical fibers. Figure 5 illustrates the output profiles of the second harmonic for the two different cases under study in this paper. For soliton formation the three beams have clean Gaussian-like profiles, as shown in Fig. 5(a). In contrast to this the output beams can be badly distorted in conventional SHG. For example, Fig. 5(b) shows the case that the input beams are focused to 100 μm at the center and the walk-off angle is 0.6 deg at a wavelength of 1092 nm. For beam waists as large as 200 and 500 μm, the beam profile of the second harmonic retains its Gaussian shape for conventional methods, even if the walk-off angle is as large as 0.6 deg. However, the fundamental fields are likely to be slightly distorted owing to the uneven depletion across the transverse profile of the beam as a function of propagation.

5. CONCLUSIONS

The features of SHG as implemented either with conventional techniques or with the generation of quadratic solitons were compared with numerical simulations. It was found that the efficiency of SHG by use of spatial-soliton formation was highly insensitive to phase mismatch and walk-off angle. If maximum conversion efficiency in noncritical phase-matching geometries is the sole criterion, then conventional approaches that utilize gentle focusing into the center of the doubling crystal are the best: quadratic soliton formation results in conversion efficiencies of the order of 10 to 20 percent. On the other hand, in cases where the soliton robustness plays a role, the soliton case has a number of attractive features. SHG accompanied by soliton formation exhibits a 3-dB detuning bandwidth at least one order of magnitude larger than for the conventional case. This reduces the usual temperature and angular tolerances normally encountered in maintaining phase matching. Furthermore, the output beam quality in cases with walk-off and large depletion is superior for the soliton case.

Finally, it should be noted that with the possibility of engineering solitons by varying the phase-matching conditions with propagation distance (i.e., periodically poled structures), the soliton's robust nature is maintained, while the SH conversion efficiency can be tailored for a particular application with values approaching 80%.[10] This, however, increases the threshold for soliton formation.

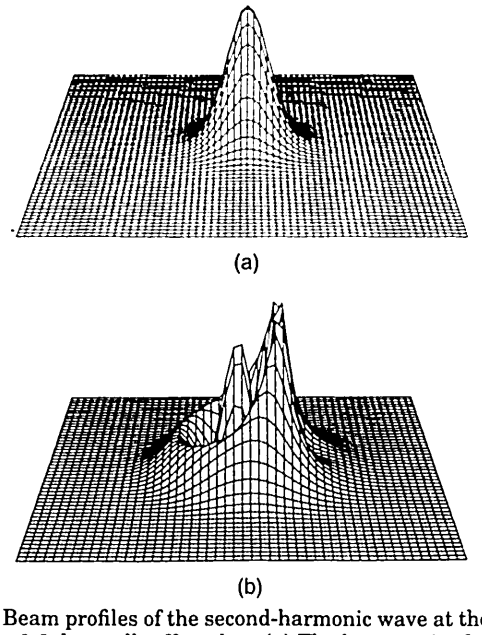

Fig. 5. Beam profiles of the second-harmonic wave at the output face for a 0.6-deg walk-off angle: (a) The beam waist for soliton generation was 20 μm, and the peak input intensity of each fundamental field was 10 GW/cm^2. (b) The 0.4-GW/cm^2 input fundamental beams for conventional SHG were focused to 100 μm at the center of the crystal.

ACKNOWLEDGMENTS

This research was supported by the National Science Foundation and AFOSR.

*Present address: Department of Biocybernetics, Faculty of Engineering, Niigata University, 8050 Ikarashi 2-no-cho, Niigata 950-2182, Japan

REFERENCES

1. R. W. Boyd, *Nonlinear Optics* (Academic, New York, 1994); P. A. Franken, A. E. Hill, C. W. Peters, and G. Weinreich, "Generation of optical harmonics," Phys. Rev. Lett. **7**, 118 (1961); J. A. Armstrong, N. Bloemergen, J. Ducuing, and P. S. Pershan, "Interactions between light waves in a nonlinear dielectric," Phys. Rev. **127**, 1918–1939 (1962).
2. K. Tatsuno, M. Takahashi, K. Muraoka, H. Sugiyama, J. Nakamura, T. Andou, and T. Miyai, "High storage density optical recording with a stable micro green second harmonic generation laser consisting of Nd:YVO_4 and KTP," Jpn. J. Appl. Phys. **31**, 601–604 (1992).
3. Reviewed recently in G. I. Stegeman, D. J. Hagan, and L. Torner, "$\chi^{(2)}$ Cascading phenomena and their applications to all-optical signal processing, mode-locking, pulse compression and solitons," J. Opt. Quantum Electron. **28** 1691–1740 (1996).
4. W. E. Torruellas, Z. Wang, D. J. Hagan, E. W. VanStryland, G. I. Stegeman, L. Torner, and C. R. Menyuk, "Observation of two-dimensional spatial solitary waves in a quadratic medium," Phys. Rev. Lett. **74**, 5036–5039 (1995).
5. L. Torner, "Stationary solitary waves with second-order nonlinearities," Opt. Commun. **114**, 136–140 (1995).
6. H. Y. Shen, Y. P. Zhou, W. X. Lin, Z. D. Zeng, R. R. Zeng, G. F. Yu, C. H. Huang, A. D. Jiang, S. Q. Jia, and D. Z. Shen, "Second harmonic generation and sum frequency mixing of dual wavelength Nd:$YALO_3$ laser in flux grown $KTiOPO_4$ crystal," IEEE J. Quantum Electron. **28**, 48–51 (1992).
7. See, e.g., G. P. Agrawal, *Nonlinear Fiber Optics* (Academic, San Diego, 1989), Chap. 2.
8. R. A. Fuerst, M. T. G. Canva, D. Baboiu, and G. I. Stegeman, "Properties of type II quadratic soliton excited by imbalanced fundamental waves," Opt. Lett. **22**, 1748–1750 (1997).
9. J. P. Feve, B. Boulanger, and G. Marnier, "Experimental study of walk-off attenuation for type II second-harmonic-generation in KTP," IEEE J. Quantum Electron. **31**, 1569–1571 (1995).
10. L. Torner, C. B. Clausen, and M. M. Fejer, "Adiabatic shaping of quadratic solitons," Opt. Lett. **23**, 903 (1998).